Nickel containing Mg-Al hydrotalcite-type anionic clay catalyst for the oxidation of alcohols with molecular oxygen

Tomonori Kawabata [a], Yuriko Shinozuka [a], Yoshihiko Ohishi [a], Tetsuya Shishido [b], Ken Takaki [a], Katsuomi Takehira [a],*

[a] *Department of Chemistry and Chemical Engineering, Graduate School of Engineering, Hiroshima University, Kagamiyama 1-4-1, Higashi-Hiroshima 739-8527, Japan*
[b] *Department of Chemistry, Tokyo Gakugei University, Koganei, Tokyo 184-3501, Japan*

Abstract

Nickel(II) containing magnesium-aluminum (3/1) hydrotalcite(HT)-type anionic clays have been prepared by co-precipitation and tested for a catalyst for liquid-phase oxidation of alcohols with molecular oxygen. The Ni substitution for the Mg site in Mg_3Al HT resulted in an appearance of the catalytic activity and the composition of $Mg_{2.5}Ni_{0.5}Al$ HT was the most effective. The oxidation of primary and secondary alcohols afforded the corresponding carbonyl compounds mainly; benzyl alcohol was the most efficiently oxidized to benzaldehyde. The yield of benzaldehyde over the hydrotalcite catalyst increased significantly with increasing nickel content up to ca. 7.6 wt%, where atomically isolated and octahedrally coordinated Ni(II) sites was effective for the oxidation with molecular oxygen. Use of non-polar solvents, such as hexane, cyclohexane, and toluene, was favorable for the oxidation reaction, among which toluene afforded the highest yield of benzaldehyde. The octahedrally coordinated Ni(II) cations incorporated inside the framework of hydrotalcite do not leach during the reaction and worked as a heterogeneous catalyst. It is considered that the Ni(II) site worked as the active site by activating molecular oxygen assisted by the Mg(II) as a base and simultaneously alcohol was activated by the Al(III) as an acid, resulting in an enhancement of the activity of the $Mg_{2.5}Ni_{0.5}Al$ HT heterogeneous catalyst for alcohol oxidation.
© 2005 Elsevier B.V. All rights reserved.

Keywords: Nickel containing Mg-Al hydrotalcite; Framework nickel; Alcohol oxidation; Molecular oxygen; Heterogeneous catalyst

1. Introduction

Catalytic oxidation of alcohols to carbonyl compounds has attracted much attention both in industrial processes and in organic synthesis [1]. Alcohols have been traditionally oxidized by non-catalytic methods with stoichiometric oxidants such as dichromate and permanganate [2]. These methods produce enormous amounts of metal salts as wastes. Much effort has been made to develop homogeneous catalytic systems to solve these problems [2,3]. However, most systems still required large quantities of additives such as NaOAc, NaOH, and K_2CO_3 [4]. There is little known about the ox-

idation of alcohols with molecular oxygen over heterogeneous catalysts. Catalytic oxidation with molecular oxygen is particularly attractive from an economical and environmental point of view [5,6]. Moreover, heterogeneous catalysts in the liquid-phase offers several advantages over homogeneous ones, such as an ease of recovery and recycling, atom utility, and enhanced stability in the oxidation reactions.

Noble metals, such as styrene-divinylbenzene copolymer anchored Ru(III) complex [7], Pd-Ag bimetallic system supported on pumice [8], Pd(II) acetate–pyridine complex supported by hydrotalcite [9], Al_2O_3 supported Ru catalyst [10], Ru hydrotalcites [11], trimetallic $Ru/CeO_2/CoO(OH)$ catalyst [12], and hydroxyapatite-bound Pd nanocluster [13] were reported to be active as heterogeneous catalysts for the oxidation of alcohols with molecular oxygen. It is likely that

the noble metals work as the catalyst probably as a Lewis acid via the peroxometal pathway. Although the use of non-noble transition metals, such as Ni and Cu, is interesting from a view point of catalytic actions by activating of molecular oxygen, such examples are not abundant in the liquid-phase oxidation of alcohols. It has been reported that an octahedral molecular sieve, synthetic manganese oxide materials with a tunnel structure, works as a heterogeneous catalyst in the oxidation of benzyl alcohol [14]. The reaction proceeded via activation of molecular oxygen through the lattice oxygen in manganese oxide associated with the Mn(IV)/Mn(II) reduction–oxidation couple. Activation of molecular oxygen on nickel in Ni-Al hydrotalcite-like anionic clay was also reported to take place in the oxidation of alcohols [15]. A wide range of alcohols, such as allylic and benzylic, and α-ketols was converted to the corresponding carbonyl compounds under mild reaction conditions by employing molecular oxygen as the stoichiometric oxidant. Moreover solvent-free oxidation of benzyl alcohol by tert-butyl hydroperoxide or molecular oxygen was successfully performed over Mn and Cu containing hydrotalcite-like anionic clays [16,17].

The most common hydrotalcite compounds consist of Mg-Al system, in which various metal cations can substitute both sites of Mg(II) and Al(III) depending on the valence state and the ionic radii [18]. When Ni(II) substitutes the Mg(II) sites, the Ni(II) will be highly dispersed and octahedrally coordinated with oxygen. If the Ni(II) species in the hydrotalcite activates molecular oxygen as suggested by Choudhary et al. [15], Mg(II) as a base could assist the reductive activation of dioxygen resulting in the acceleration in the alcohol oxidation. In the present paper, we report the catalytic behavior of Ni(II) containing Mg-Al hydrotalcite-like anionic clay in the oxidation of alcohols with molecular oxygen. Surface amount of Ni effective for the oxidation reaction was evaluated by a novel method using NaOCl as an oxidant. Various alcohols were oxidized with a coupled system of O_2/Mg(Ni)-Al hydrotalcite and, moreover, the crystal structures and coordination environments of the introduced nickel species are characterized to obtain information concerning the working mechanism.

2. Experimental

2.1. Catalyst preparation

Ni containing Mg-Al hydrotalcite, $[Mg(II)_{1-x}Al(III)_x (OH)_2]^{x+}(CO_3^{2-}{}_{x/2})\cdot nH_2O$, in which a part of Mg(II) was replaced by Ni(II), were prepared by co-precipitation method reported by Miyata and Okada [19] with minor modification. An aqueous solution of the nitrates of Mg(II), Ni(II) and Al(III) was added slowly with vigorous stirring into an aqueous solution of sodium carbonate at 333 K. By adjusting the pH of this solution to 10 with an aqueous solution of sodium hydroxide, heavy slurry precipitated. The crystal growth took place by aging the solution at 333 K for 24 h. After the solution was cooled to room temperature, the precipitate was washed with distilled water and dried in air at 383 K for 12 h. Ni-Al hydrotalcite as a control was also prepared in a similar way. A list of these catalysts is shown in Table 1.

Table 1
Oxidation of benzyl alcohol over Ni containing Mg-Al hydrotalcite[a]

Entry	Catalyst[b]	(Mg+Ni)/Al ratio	Ni (wt%)[c]	BET surface area/m² g_{cat}^{-1}	Benzyl alcohol conversion (%)	Benzaldehyde		TON[d]		
						Selectivity (%)	Yield (%)	Total Ni	NaOCl	NaOCl[e]
1	None	–	–	–	2.2	69.5	1.5	–	–	
2	Mg₃Al HT	3	–	91.3	9.3	0	0	–	–	
3	Ni₂Al HT	2	34.6	99.9	48.6	66.5	32.3	0.2	5.0	3.1
4	Ni₂Al HT*	2	34.9	119.9	65.4	83.3	54.5	0.4	–	
5	Ni₃Al HT	3	38.2	117.7	52.3	78.2	40.9	0.2	3.0	2.9
6	Ni₃Al HT*	3	38.0	98.2	69.0	81.4	56.2	0.5	–	
7	Ni₃Al HT**	3	40.2	24.0	15.1	84.1	12.7	0.1	0.2	
8	Mg₂.₉Ni₀.₁Al HT	3	1.3	80.1	16.0	2.5	0.4	0.1	0.2	–
9	Mg₂.₇₅Ni₀.₂₅Al HT	3	3.7	74.6	21.6	51.7	11.6	0.7	4.6	0.5
10	Mg₂.₅Ni₀.₅Al HT	3	7.6	121.2	51.8	97.8	50.6	1.6	18.5	18.5
11	Mg₂NiAl HT	3	14.6	106.3	50.4	78.6	39.6	0.6	9.7	7.9
12	Mg₀.₇₅Ni₀.₂₅Al HT	1	8.2	95.4	16.7	6.0	1.0	0.4	–	
13	Mg₁.₇Ni₀.₃Al HT	2	6.9	94.0	16.9	39.6	6.7	0.4	–	
14	Mg₃.₅₅Ni₀.₄₅Al HT	4	7.1	86.7	14.0	22.1	3.1	0.5	–	
15	imp-Ni/γ-Al₂O₃	–	7.6	98.0	9.4	7.0	0.7	0.0	0.0	
16	imp-Ni/MgO	–	7.6	47.5	8.1	34.6	2.8	0.1	0.1	

[a] Catalyst, 0.5 g; benzyl alcohol, 2 mmol; toluene, 10 ml; O_2, 6 ml min^{-1}; reaction temperature, 333 K; reaction time, 6 h.
[b] Prepared by co-precipitation method without pH control*; by hydrothermal method at 463 K**.
[c] Measured by ICP.
[d] Calculated based on the total amount of Ni or by the NaOCl method.
[e] The amount of catalyst was normalized so as to contain 0.648 mmol of Ni in the catalyst.

Also as controls, two types of Ni-Al hydrotalcite were prepared following the methods reported by Choudhary et al. [15] and Reichle [20], i.e., co-precipitation at ambient temperature followed by stirring at 338 K for 18 h and by vacuum drying at 383 K (shown by '*' in Table 1) and co-precipitation at 303 K followed by hydrothermal treatment at 463 K for 18 h in autoclave and by vacuum drying at 383 K (shown by '**' in Table 1). In both cases, pH in the solution was not controlled during the co-precipitation. Moreover, the catalysts as references were prepared by conventional impregnation (*imp*) using γ-Al_2O_3 and MgO as the carrier. Loading amount of Ni was fixed at 7.6 wt% on both catalysts after the drying in air at 383 K for 12 h.

2.2. Characterization of the catalyst

The structures of the catalysts were studied by XRD, MAS-NMR, TG-DTA, SEM, ICP, UV–vis, N_2-adsorption, and TPR methods. Powder X-ray diffraction (XRD) measurements were performed with a Rigaku powered diffraction unit, RINT2250VHF with Cu Kα radiation (40 kV, 300 mA). The diffraction patterns were identified by comparing with those included in the JCPDS (Joint Committee of Powder Diffraction Standards) database. MAS (magic-angle spinning) ^{27}Al NMR (nuclear magnetic resonance) spectra were obtained using a Bruker AMX 400 spectrometer at a magnetic field of 9.4 T. The spectra were recorded at a resonance frequency of 104.26 MHz and a rotor-spinning rate of 3 kHz. The pulse length was 1.0 μs. For each spectrum, 128 scans were accumulated. Chemical shifts are given relative to a 1 M aqueous aluminum nitrate solution. TG-DTA was recorded under air with a Shimadzu TGA-50 and DTA-50 analyzer using 10 mg of sample and at a rate of 10 K min^{-1}. Scanning electron micrograph (SEM) was obtained on a JEOL JSM-6340F instrument equipped with a Link SATW EDS. The ICP measurements were carried out using a Perkin-Elmer OPTIMA 3000. The content of metal component was determined after the sample was completely dissolved using diluted hydrochloric acid and a small amount of hydrofluoric acid. The diffuse reflectance UV–vis spectra were recorded on a JASCO UV/VIS/NIR (V-570) spectrophotometer. The powdery sample was loaded into a quartz cell, and the spectra were collected at 200–700 nm referenced to $BaSO_4$. N_2-adsorption (77 K) data obtained with a Bell Japan BEL-SORP 18SP equipment (volumetric) were used to examine both BET surface areas and the properties of mesopores of the Mg-Ni-Al hydrotalcite. The pore size distribution was evaluated from the adsorption isotherm by the DH (Dollimore-Heal) method [21]. The Ni K-edge X-ray absorption spectra were measured in a transmission mode at the EXAFS facilities installed at BL-7C line of KEK-PF, Tsukuba, Japan. Data reductions were performed with the FACOM M1800 computer system of the Data Processing Center of Kyoto University [22] The sample was mixed with boron nitride as a binder and pressed into a disk (Ø10 mm). Energy was calibrated with Cu K-edge absorption (8981.0 eV), and the energy step of measurement in the XANES region was 0.3 V. The adsorption was normalized to 1.0 at an energy position of 30 eV higher than the adsorption edge. Temperature programmed reduction (TPR) of the catalyst was performed with 50 mg of the catalyst at a heating rate of 10 K min^{-1} using a mixture of 5 vol% H_2/Ar (100 ml min^{-1}) as reducing gas. A TCD was used for monitoring the H_2 consumption after passing through a 13× molecular sieve trap to remove water. Prior to the TPR measurements, the sample was treated at 573 K for 1 h in 20 vol% O_2/Ar gas (50 ml min^{-1}).

2.3. Catalytic reactions

Benzyl alcohol (>98%), 4-methoxybenzyl alcohol (>98%), 4-bromobenzyl alcohol (>98%), 2-phenylethanol (>98%), cinnamyl alcohol (>98%), and 1-octanol (>98%) (Wako Pure Chemical Industries) were used as reactants without further purification. The oxidation of alcohol was carried out using a Pyrex batch-type reactor equipped with a reflux condenser. In a typical reaction, 0.5 g of catalyst was added to glass flask pre-charged with 2 mmol of alcohol and 10 ml of solvent at 333 K. The reaction was started by bubbling O_2 gas through the reactor at a rate of 6 ml min^{-1} under vigorous stirring. After the reaction, the catalyst was filtrated and a small part of the dried catalyst was subjected to the analyses. All liquid organic products were identified by GC–MS (Shimadzu GCMS-QP5050) and were quantified using a gas chromatograph with a capillary column (BPX-5, 30 M × 0.25 mmφ) and a FID detector using cyclohexanone as an internal standard.

Turnover number of surface Ni site was obtained by a method in which NaOCl was used as an oxidizing agent of surface Ni on the catalysts. 10 ml of 6% NaOCl aqueous solution containing 1.4 g NaOH was slowly added into 40 ml of water containing 2 g of the supported Ni catalyst at 293 K. The solution was stirred for 30 min at 293 K and the precipitate was washed with 1 L of distilled water and vacuum dried at 313 K for 12 h. After the treatment, the catalyst became darkened in color, suggesting that the surface Ni was converted to the higher oxidized state. The catalyst (0.5 g) was used for the oxidation of benzyl alcohol and the amount of benzaldehyde formed was analyzed. The reaction was carried out in N_2 atmosphere, where no oxidation of benzyl alcohol took place over non-treated catalyst. Assuming that all active Ni species on the catalyst surface was peroxidized and in turn stoichiometrically oxidize benzyl alcohol to benzaldehyde, the number of surface active Ni sites could be evaluated from the amount of benzaldehyde formed. Finally, the turnover number (TON) was calculated by comparing the molar amount of benzaldehyde formed in the oxidation with the number of active Ni sites on the supported Ni catalysts.
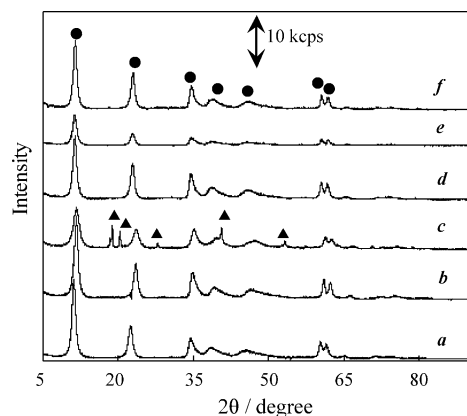
Fig. 1. X-ray diffraction patterns of the Mg-Ni-Al catalysts. (a) $Mg_{3.55}Ni_{0.45}Al$ HT, (b) $Mg_{1.7}Ni_{0.3}Al$ HT, (c) $Mg_{0.75}Ni_{0.25}Al$ HT, (d) Ni_3Al HT, (e) Mg_2NiAl HT, (f) $Mg_{2.5}Ni_{0.5}Al$ HT, (g) $Mg_{2.75}Ni_{0.25}Al$ HT and (h) Mg_3Al HT. (●), hydrotalcite; (▲), $Al(OH)_3$.

3. Results and discussion

3.1. Crystal structure of the catalysts

XRD patterns of Ni catalysts are shown in Figs. 1 and 2. All samples in Fig. 1 were prepared by co-precipitation at a constant pH of 10 and showed typical patterns of hydrotalcite; i.e., a set of three reflection lines at $2\theta = 11.3$, 22.7 and 34.5° appeared, suggesting that the materials possess a layered structure, in which both Ni(II) and Al(III) substituted the Mg(II) sites in the brucite-like sheets [16]. Intensities of reflection lines of hydrotalcite varied depending on Ni content in Mg(Ni)Al HT at a constant (Mg + Ni)/Al ratio of 3/1 (Fig. 1d–f), among which the weakest line intensity of Mg(Ni)-Al HT was observed for $Mg_{2.5}Ni_{0.5}Al$ HT. This indicates that the crystal size was the smallest for $Mg_{2.5}Ni_{0.5}Al$ HT, probably relating to the high surface area of $Mg_{2.5}Ni_{0.5}Al$ HT (Table 1, entry 10). When the ratio of (Mg + Ni)/Al was changed (Fig. 1a–c), the formation of $Al(OH)_3$ as observed for the sample $Mg_{0.75}Ni_{0.25}Al$ HT. This is due to a well-

known fact that the Mg/Al ratio below 2 is not favorable for the formation of hydrotalcite structure [18].

The line intensities of Ni_3Al HT significantly varied depending on the preparation method (Fig. 2), i.e., the most highly crystallized structure was obtained by co-precipitation followed by hydrothermal treatment (Fig. 2b), then by co-precipitation under controlled pH (Fig. 2c) and finally by co-precipitation under non-controlled pH (Fig. 2a). In fact, the size of crystallites calculated from the line width of reflection (0 0 3) for three samples was as follows: Ni_3Al HT*, 21.9 nm; Ni_3Al HT, 9.5 nm and Ni_3Al HT**, 8.9 nm. A similar calculation for the sample of $Mg_{2.5}Ni_{0.5}Al$ HT (Fig. 1b) showed the value of 11.0 nm as the crystallite size. The sizes of periclase Mg(Al)O after the calcinations of Mg-Al HT at 423 and 723 K were reported to be 5.0 [23] and 3.8 nm [24], respectively.

TPR of Ni_3Al HT showed a strong peak of H_2 consumption around 773 K together with a weak peak at 623 K. With increasing the amount of Mg replaced by Ni in Ni_3Al HT, both peaks shifted toward higher temperature. As a result, the former was observed at 1213 K while the latter was at 733 K for $Mg_{2.9}Ni_{0.1}Al$ HT, with decreasing intensities of both peaks. It is considered that, during the TPR, Mg(Ni)-Al HT was dehydrated and decomposed to form finally periclase Mg(Ni,Al)O around 675 K (*vide infra*). It was confirmed by the XRD analysis that Ni_3Al HT was decomposed to form NiO (JCPDS 40835) after the calcination at 773 K for 1 h and no reflection lines of Al containing species was observed. This suggests that Al is included in NiO as Ni(Al)O solid solutions. Therefore, the former peak observed at high temperature is attributed to the reduction of Ni(II) in Ni(Al)O or periclase Mg(Ni,Al)O, while the latter observed at low temperature is attributed to the reduction of Ni(II) in isolated NiO. Increase in the reduction temperature is probably due to the stabilization of Ni(II) incorporated in periclase Mg(Al)O by the formation of solid solutions as Mg(Ni,Al)O; this stabilization effect could increase with increasing ratio of Mg/Ni.

3.2. Morphology and pore structure of the catalysts

SEM image of $Mg_{2.5}Ni_{0.5}Al$ HT is shown in Fig. 3. After drying the precipitates obtained by co-precipitation at 358 K, the "card house" structure was clearly observed. Each card has a size of 100–300 nm in diameter and 20 nm in thickness by the observation at high magnification and probably consisted of the $Mg_{2.5}Ni_{0.5}Al$ HT layered structure. The DTA/TGA curves of $Mg_{2.5}Ni_{0.5}Al$ HT showed two notable endothermic peaks accompanied by significant weight loss at 487 and 675 K as T_{max}. These temperatures were fairly lower compared with the values of 543 and 720–740 K observed for pure Mg_3Al HT [18], suggesting that the Mg_3Al HT structure became unstable by the introduction of Ni(II) in the Mg(II) sites. The former endothermic peak corresponds to the loss of interlayer water, whereas the latter does to multiple phenomena; i.e., the hydroxyl groups bound to Al, then those of $Mg(OH)_2$ are lost and finally the carbonate decomposes.
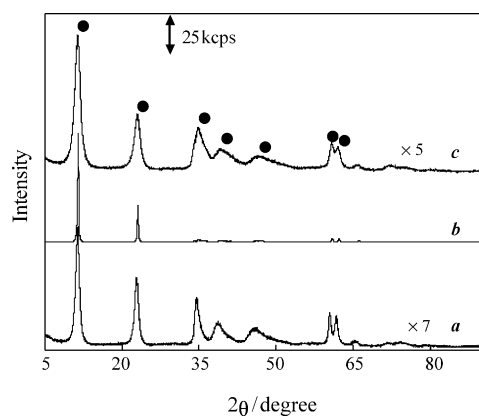

Fig. 2. X-ray diffraction patterns of the Ni-Al catalysts. (a) Ni_3Al HT, (b) Ni_3Al HT** and (c) Ni_3Al HT*. (●), hydrotalcite.
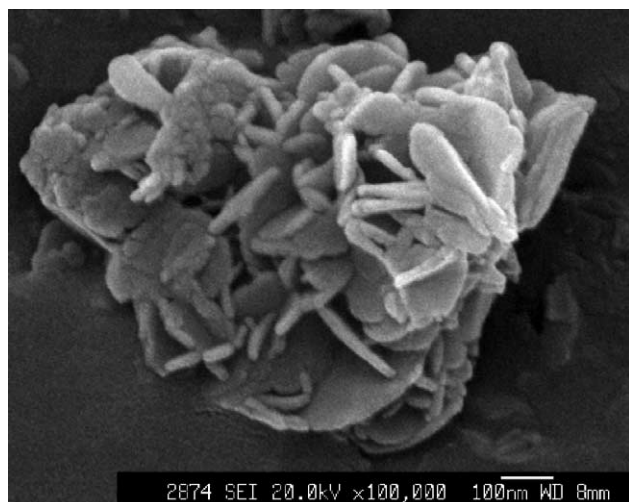
Fig. 3. SEM image of $Mg_{2.5}Ni_{0.5}Al$ HT.

Fig. 4. Normalized Ni K-edge XANES spectra of the catalysts. (a) $Mg_{2.5}Ni_{0.5}Al$ HT, (b) NiO and (c) Ni foil.

Final products will be periclase Mg(Ni,Al)O, in which not only Ni(II) but also Al(III) replaced the Mg(II) sites [25].

It is considered that no substantial change in the $Mg_{2.5}Ni_{0.5}Al$ HT structure took place after the drying in air at 373 K for 24 h, except the loss of water weakly bound to the hydrotalcite, during the catalyst preparation. Pore distribution of the $Mg_{2.5}Ni_{0.5}Al$ HT showed a peak around 2–3 nm together with wide distribution up to 20 nm in radius. The lowest limit of pore radius detectable in the present method is 2 nm, and therefore the information concerning micropores smaller than 2 nm could not be obtained. However, SEM images clearly showed a card-like structure probably derived from the layered hydrotalcite structures, suggesting that micropores must exist in the samples. The former pore sizes are related to the layered structure, while the latter is due to the "card house" structure consisting of many small plates [25]. We calculated the basal interlayer spacing from the strong symmetric (0 0 3) reflection ($2\theta = 13.4°$) of Mg-Al (3/1) hydrotalcite. If the thickness of the brucite-like layer is assumed to be 4.8 Å [26], the interlayer distance corresponds to 2.9 Å. It is concluded that $Mg_{2.5}Ni_{0.5}Al$ HT possesses a porous structure consisting of various sizes of micro- and mesopores.

Surface area of the catalyst varied substantially depending on the Ni contents in Mg(Ni)-Al HT (Table 1). In a series of $Mg_{3-x}Ni_xAl$ HT, surface area increased with increasing Ni content up to 7.6 wt% ($Mg_{2.5}Ni_{0.5}Al$ HT) and a further increase in Ni content resulted in a decrease in the surface area (Table 1, entries 8–11). Increase in the Mg/Al ratio at a constant Ni content of 7.6 wt% resulted in a decrease in the surface area (Table 1, entries 10 and 12–14). Surface area of Ni-Al HT varied drastically depending on the preparation method. Hydrothermal treatment afforded a rather small surface area as observed for Ni_3Al HT**, probably due to its highly crystallized structure. In contrast, the surface area increased by co-precipitation under non-controlled pH as seen for Ni_2Al HT*, and further increased by controlling pH in co-
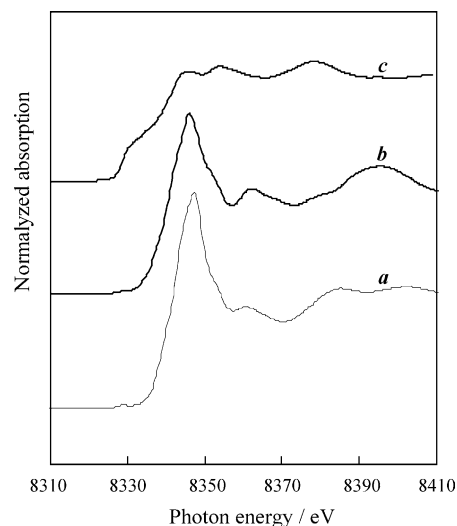
precipitation of Ni_3Al HT, possibly due to the formation of small particles. Both samples, Ni_3Al HT** and Ni_2Al HT*, were prepared under different aging treatments in order to trace the catalytic results obtained by Choudhary et al. [15].

3.3. Coordination structure around Ni(II) in the catalysts

Fig. 4 shows Ni K-edge X-ray absorption near-edge structure (XANES) spectra of $Mg_{2.5}Ni_{0.5}Al$ HT together with reference compounds such as NiO and Ni foil. The XANES spectrum of $Mg_{2.5}Ni_{0.5}Al$ HT (Fig. 4a) resembles that of the NiO (Fig. 4b) with an octahedral coordination environment [27], but differs from that of Ni foil (Fig. 4c) in shape and edge position. The absence of a pre-edge peak due to the 1s–3d transition near 8333 eV [28] strongly suggests that the Ni(II) cations in $Mg_{2.5}Ni_{0.5}Al$ HT occupy only octahedral sites. Similar discussions concerning Ni coordination are also reported by Feth et al. [29] and Kwag et al. [30]. The Fourier transforms (FT) of k^3-weighted extended X-ray absorption fine structure (EXAFS) is depicted in Fig. 5. The peak at 1.7 Å (non-phase-shift corrected) observed for both $Mg_{2.5}Ni_{0.5}Al$ HT (Fig. 5a) and NiO (Fig. 5b) was assignable to a Ni-O moiety [31]. By the calculations of EXAFS parameters of $Mg_{2.5}Ni_{0.5}Al$ HT (Fig. 5a), the coordination number (*CN*) and distance for the Ni-O shell of the Ni(II) species in the hydrotalcite are estimated at 6 and 2.09 Å, respectively. They are in good agreement with those of XANES data. A broad peak near 2.6 Å (non-phase-shift corrected) can be assigned to the mixture of Ni–(O)–M (M = Ni, Al, and Mg) [32] and its intensity is considerably weak in comparison with that of NiO ($CN_{Ni-(O)-Ni} = 12$) [33]. Therefore, it is reasonable to consider that Ni(II) species in $Mg_{2.5}Ni_{0.5}Al$ HT is highly dispersed.

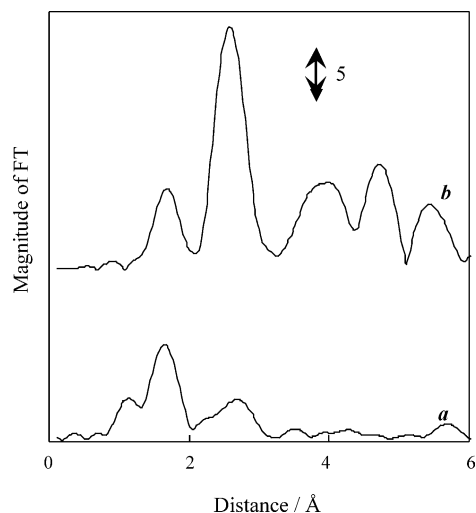The diffuse-reflectance UV–vis spectra of Ni containing Mg-Al hydrotalcite together with a control catalyst such as

Fig. 5. Fourier transforms of k^3-weightened Ni K-edge EXAFS of the catalysts. (a) $Mg_{2.5}Ni_{0.5}Al$ HT and (b) NiO. Phase shift was not corrected.

imp-Ni/γ-Al$_2$O$_3$ have been also recorded (Fig. 6). The spectra are highly similar for all Mg(Ni)-Al HT samples (Fig. 6c–g), with two split broad bands with two pairs of maxima at 740, 655 and 410, 380 nm, while both samples of *imp*-Ni/γ-Al$_2$O$_3$ and *imp*-Ni/MgO showed spectra shifted toward higher wave length (Fig. 6a and b). As both Mg(II) and Al(III) have d^0 configurations, all bands recorded (in addition to those higher energy, due to charge transfer processes) should be ascribed to d–d transition in the octahedrally coordinated Ni(II) cation as reported by Holgano et al. [34]. Schoonheydt et al. [35] and Briend-Faure et al. [36] observed the bands at 620 and 560 nm in the zeolite-supported Ni and assigned them to Ni(II) in a tetrahedral symmetry. Moreover, Lepetit and Che [37] and Zanjanchi and Ebrahimian [38] reported that the bands at about 475 nm and a peak on its shoulder at ∼445 nm for the
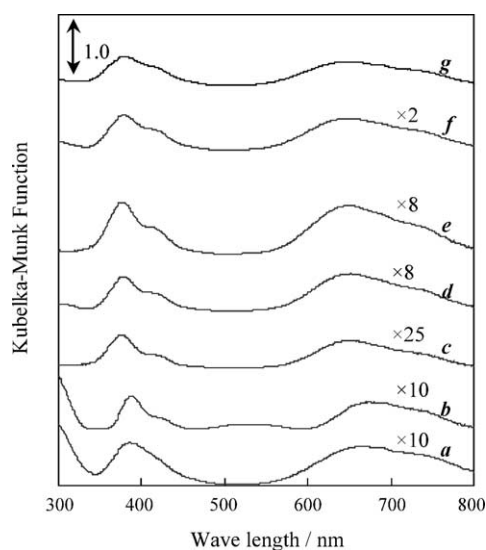

Fig. 6. Diffuse reflectance UV–vis spectra of the catalysts. (a) *imp*-Ni/γ-Al$_2$O$_3$, (b) *imp*-Ni/MgO, (c) $Mg_{2.9}Ni_{0.1}Al$ HT, (d) $Mg_{2.75}Ni_{0.25}Al$ HT, (e) $Mg_{2.5}Ni_{0.5}Al$ HT, (f) Mg_2NiAl HT and (g) Ni_3Al HT.

samples of nickel-exchanged zeolites were assigned to Ni(II) in a distorted tetrahedral position. These absorption bands at 620, 560, 475, and ∼445 nm were not observed in the present samples, indicating that Ni(II) is octahedrally coordinated in Mg(Ni)-Al HT. Both *imp*-Ni/γ-Al$_2$O$_3$ and *imp*-Ni/MgO were prepared by impregnation of the supports with Ni(II) nitrate in aqueous solution, followed by drying at 383 K. Ni(II) compound probably exists on the catalyst surface, and the coordination around Ni(II) is difficult to be discussed. MAS ^{27}Al NMR of Mg-Al HT as prepared showed a resonance line at 8.8 ppm assigned to Al(III) octahedrally coordinated to oxygen. $Mg_{2.9}Ni_{0.1}Al$ HT showed almost similar resonance line, indicating that Al(III) is coordinated octahedrally regardless of the presence of Ni(II) at the Mg(II) site.

3.4. Oxidation of benzyl alcohols

Table 1 shows the results of oxidation of benzyl alcohol with various supported Ni catalysts along with control catalysts. In the absence of catalyst, benzyl alcohol oxidation afforded only small amount of benzaldehyde. Small amount of benzyl alcohol was consumed but benzaldehyde was not produced with Mg$_3$Al HT. Both Ni/γ-Al$_2$O$_3$ and Ni/MgO catalysts prepared by impregnation showed low activity, among which the latter was slightly effective for the production of benzaldehyde, suggesting that MgO as a base assisted the alcohol oxidation on Ni(II). The incorporation of Ni in Mg-Al HT or the formation of NiAl HT resulted in an appearance of good catalytic activity. $Mg_{2.5}Ni_{0.5}Al$ HT revealed the highest activity among both series of Mg(Ni)-Al HT catalysts with various Ni contents at a constant (Mg + Ni)/Al ratio of 3/1 (Table 1, entries 8∼11) and with varying (Mg + Ni)/Al ratios at a constant Ni content of 7.6 wt% (Table 1, entries 10 and 12–14). Surface area was the highest for $Mg_{2.5}Ni_{0.5}Al$ HT among both series of catalyst. It is likely that the activity substantially depended on the surface area as well as the Ni content of the catalyst. Blank tests in the absence of O$_2$ always showed the benzyl alcohol conversion of ca. 10% over Mg$_{3-x}$Ni$_x$Al HT catalysts, suggesting that a substantial amount of benzyl alcohol is adsorbed on the catalyst surface. The adsorption of benzyl alcohol probably took place in the layers of all HT catalysts irrespective of the Ni content, and therefore the selectivity to benzaldehyde apparently decreased at the low benzyl alcohol conversion. Small amounts of benzoic acid and benzyl benzoate were formed as by-products.

Choudhary et al. [15] reported that Ni$_2$Al HT catalyzes the oxidation of various kinds of alcohols, such as α-ketols, benzylic alcohols, and allylic alcohols, to the corresponding carbonyl compounds, among which substituted benzyl alcohols as well as secondary benzylic alcohols were oxidized almost quantitatively. However benzyl alcohol was not oxidized efficiently and the yield of benzaldehyde was 31% after the reaction for 12 h [15]. In the present study, Ni$_2$Al HT, Ni$_2$Al HT*, Ni$_3$Al HT and Ni$_3$Al HT* showed high values in both benzyl alcohol conversion and benzaldehyde

selectivity except for Ni$_3$Al HT** with a small surface area. This is probably due to their high Ni contents in the catalyst. The activity can be precisely compared by TON, i.e., turnover number, calculated based on total Ni amount in the catalyst (vide infra). Judging from TON, benzyl alcohol was most efficiently oxidized to benzaldehyde on Mg$_{2.5}$Ni$_{0.5}$Al HT (Table 1, entry 10).

3.5. Turnover number in oxidation of benzyl alcohol

Precise comparison of the activity of each catalyst must be done for the TON of active Ni site. All catalysts prepared in the present work contain Ni species uniformly dispersed in the bulk of catalyst particles except those prepared by impregnation. Tentatively, TON of each catalyst was calculated based on total amount of Ni and shown in Table 1. Evidently Ni incorporation in Mg-Al HT structure was favorable for increasing TON of the catalyst. The highest value was obtained with Mg$_{2.5}$Ni$_{0.5}$Al HT, followed by Mg$_{2.0}$Ni$_{1.0}$Al HT and Mg$_{2.75}$Ni$_{0.25}$Al HT, suggesting an importance of high surface area of Mg$_{2.5}$Ni$_{0.5}$Al HT for the activity. Among the catalysts tested, the highest selectivity to benzaldehyde was obtained also with Mg$_{2.5}$Ni$_{0.5}$Al HT. However, substantial amount of Ni cannot work in these catalysts and therefore a more precise study on the activity of active Ni site is necessary. The TON obtained by the NaOCl method is also shown in Table 1. It was reported that NaOCl can oxidizes Ni(OH)$_2$ to form a higher valent NiO [39–41] or a Ni peroxide [42,43] both of which oxidize various organic compounds. Physico-chemical properties of the higher valent NiO have been well established, while those of the Ni peroxide have not been done. The higher valent NiO possess Ni(IV) as well as active oxygen (O*) on the surface and can be shown as (HO)$_2$Ni=O*·mH$_2$O. The higher valent NiO stoichiometrically oxidizes benzyl alcohol as follows:

$$PhCH_2OH + (HO)_2Ni=O^*$$
$$\rightarrow PhCHO + H_2O + (HO)_2Ni \qquad (1)$$
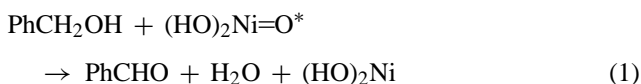
If the Ni species located on the surface of the catalyst particle is oxidized by NaOCl to the higher valent NiO, which in turn oxidizes stoichiometrically benzyl alcohol to benzaldehyde. Moreover, if such Ni species are active also for the benzyl alcohol oxidation with molecular oxygen, the TON obtained by NaOCl method must be reliable for comparing the activity of Mg(Ni)-Al HT catalyst.

Effect of the amount of NaOCl added in the oxidation of benzyl alcohol over Mg$_{2.5}$Ni$_{0.5}$Al HT was examined (Fig. 7). The reaction was carried out using 1 mmol of benzyl alcohol, 0.25 g of Mg$_{2.5}$Ni$_{0.5}$Al HT and 5 ml of toluene as solvent at 333 K for 6 h. With increasing amount of 6% NaOCl aqueous solution up to 0.18 ml, yield of benzaldehyde linearly increased and reached ca. 2.0%. Further increase in the amount of NaOCl showed a slow increase in the benzaldehyde yield, suggesting that the all surface Ni was already converted to the higher valent NiO and excess NaOCl did not work as
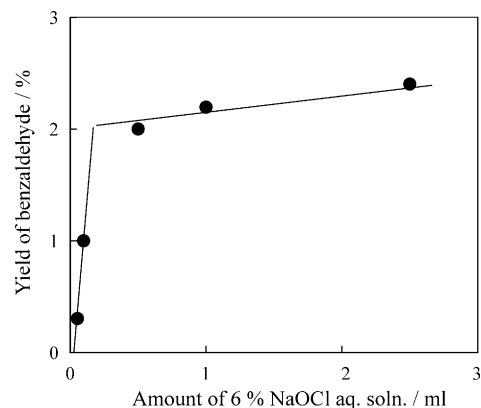

Fig. 7. Effect of the amount of NaOCl in the stoichiometric oxidation of benzyl alcohol over Mg$_{2.5}$Ni$_{0.5}$Al HT.

the oxidant. At the intersecting point, the yield of benzaldehyde was ca. 2% and the amount of 6% NaOCl added was 0.18 ml. Therefore, 0.04 mmol of benzaldehyde was formed by consuming 0.145 mmol of NaOCl, suggesting that only 27.6% of NaOCl consumed was used for the formation of active higher Ni oxide. Moreover, 0.5 g of Mg$_{2.5}$Ni$_{0.5}$Al HT contained 0.647 mmol of Ni, while the amount of active Ni on the surface was 0.04 mmol judging from the amount of benzaldehyde formed. As a result, it is concluded that 6.2% of total Ni in the Mg$_{2.5}$Ni$_{0.5}$Al HT catalyst was effective for the oxidation reaction.

Usually 10 ml of 6% NaOCl aqueous solution was used in the pre-treatment of 2 g of the catalyst for the oxidation of 2 mmol of benzyl alcohol in 10 ml of toluene at 333 K for 6 h. Use of the excess amount of NaOCl compared with 0.18 ml of 6% NaOCl solution for 0.25 g of catalyst at the intersecting point (Fig. 7) probably resulted in reliable results in the calculation of TON as shown in Table 1. When 0.5 g of catalyst was used, Mg$_{2.5}$Ni$_{0.5}$Al HT showed the highest TON, followed by Mg$_{2.0}$Ni$_{1.0}$Al HT and Mg$_{2.75}$Ni$_{0.25}$Al HT. Both Ni$_2$Al HT and Ni$_3$Al HT showed relatively high values. Almost similar order of the TON was obtained when the amount of catalyst was normalized so as to contain the same amount of Ni in the catalyst. Mg$_{2.75}$Ni$_{0.25}$Al HT showed small TON values probably due to a use of the large amount of catalyst, resulting in an inutile adsorption of benzyl alcohol or benzaldehyde (vide infra). In the oxidation of benzyl alcohol using molecular oxygen, the following TON values were reported, i.e., 8.8 after 8 h reaction in toluene with hydrotalcite-supported Ru catalyst [11], 40 after 1 h reaction in trifluorotoluene with Ru/Al$_2$O$_3$ catalyst [10], 9800 after 1 h reaction in trifluorotoluene with hydroxyapatite-supported Pd nanocluster catalyst [13], and 19.6 after 3 h reaction in toluene with hydrotalcite-supported Pd catalyst [9]. All these catalysts contain precious metals, such as Pd and Ru, on the surface, whereas the catalyst in the present work consisted of Ni, non-precious metal, as the active species. Chaudhary et al. [15–17] reported that Ni-hydrotalcites catalyze the oxidation of benzyl alcohol in the presence of molecular oxygen; however, no detailed data

Table 2
Effect of solvent in the oxidation of benzyl alcohol over $Mg_{2.5}Ni_{0.5}Al$ HT[a]

Run number	Solvent	Benzyl alcohol	Benzaldehyde	
		Conversion (%)	Selectivity (%)	Yield (%)
1	Hexane	54.0	61.9	33.4
2	Cyclohexane	57.9	67.3	38.9
3	Toluene	51.8	97.8	50.6
4	Acetonitrile	13.4	26.6	3.5
5	Tetrahydrofuran	16.4	64.6	10.4
6	Ethyl acetate	14.7	16.4	2.3

[a] Catalyst, 0.5 g; benzyl alcohol, 2 mmol; solvent, 10 ml; O_2, 6 ml min^{-1}; Reaction temperature, 333 K; reaction time, 6 h.

concerning the specific activity, TON, was shown. This is the first paper clarifying the catalytic cycles of Ni containing hydrotalcite in the oxidation of benzyl alcohol by molecular oxygen as the oxidant.

3.6. Oxidation of various alcohols in various solvents

The results of benzyl alcohol oxidation over $Mg_{2.5}Ni_{0.5}Al$ HT catalyst in various solvents are shown in Table 2. Use of polar solvents such as acetonitrile, tetrahydrofuran, and ethyl acetate afforded poor results, whereas non-polar solvents such as hexane, cyclohexane, and toluene showed a favorable effect in benzyl alcohol oxidation, among which toluene produced the most favorable effect. These results are almost similar to those obtained over Ni-Al HT as the catalyst by Choudhary et al. [15]. Polar solvents can be more strongly adsorbed than non-polar solvents on the active sites on the catalyst surface and prevent the adsorption of alcohols, resulting in the lowering in the reaction rate.
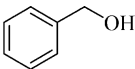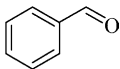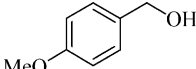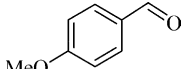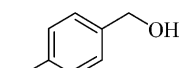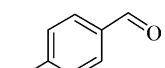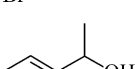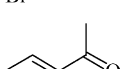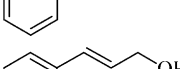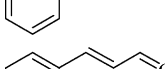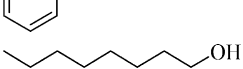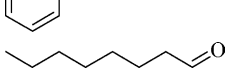
The $Mg_{2.5}Ni_{0.5}Al$ HT was proved to be the best catalyst in the present study, and was further evaluated in the oxidation of various kinds of alcohols (Table 3). Benzyl alcohol was the most quickly oxidized to benzaldehyde, whereas 4-substituted benzyl alcohols were slowly oxidized to the corresponding benzaldehydes. Secondary benzylic alcohol was also oxidized at a slower rate than primary ones. These observations are in contrast to the results reported using Ni-Al HT by Choudhary et al. [15], and rather similar to those obtained by Kaneda et al. [11] using Ru HT, wherein primary benzylic alcohols were oxidized at the faster rate than the others. Cinnamyl alcohol was mainly oxidized to cinnamaldehyde together with a small amount of benzaldehyde, suggesting that C=C double bond was attacked in the present reaction. No oxidation took place for linear alcohol such as 1-octanol.

Almost all alcohols tested in the present work showed the value of ca. 10% as a difference between the alcohol conversion and the yield of carbonyl compound. It is likely that the oxidation reaction proceeds as follows: alcohol is first absorbed in the layered structure and adsorbed on the active Ni sites, where the alcohol oxidation takes place to form the corresponding carbonyl compound. When the catalyst is not active enough, the absorbed alcohol cannot be oxidized and remains in the layered structure, resulting in the lowering in the selectivity. As seen in the result of blank test for benzyl alcohol, ca. 10% of alcohol seems to have been absorbed and remained in the HT layer without having been oxidized in all reactions.

3.7. Evidence of heterogeneous catalysis

Time course of the oxidation of benzyl alcohol over $Mg_{2.5}Ni_{0.5}Al$ HT in toluene is shown in Fig. 8. The yield

Table 3
Oxidation of alcohols over Mg_2 5M0 5AI HT[a]

Run number	Alcohol	Reaction time (h)	Conversion (%)	Product	Yield (%)
1		6	51.8		50.6
2		6	15.2		14.3
		24	64.5		51.9
3		6	20.6		14.1
		24	50.9		37.1
4		6	21.3		13.0
		24	55.0		45.9
5		6	23.9		11.9[b]
		24	31.1		15.0[c]
6		6	0.0		0.0

[a] $Mg_{2.5}Ni_{0.5}Al$ HT, 0.5 g; alcohol, 2 mmol; toluene, 10 ml, O_2, 6 ml min^{-1}, reaction temperature, 333 K.
[b] 1.1% of benzaldehyde was formed.
[c] 1.4% of benzaldehyde was formed.
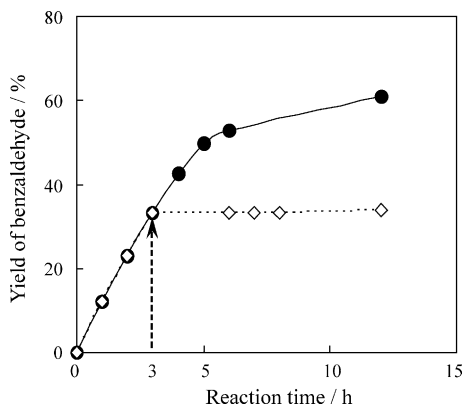
Fig. 8. Evidence of heterogeneous catalysis of $Mg_{2.5}Ni_{0.5}Al$ HT in the oxidation of benzyl alcohol. Catalyst, 0.5 g; Toluene, 10 ml; Benzyl alcohol, 2 mmol; O_2, 6 ml min^{-1}; Reaction temperature, 60 °C (●), Continuous reaction; (◇), Catalyst was removed by filtration after 3 h of the reaction.

Fig. 9. Proposed mechanism for the alcohol oxidation.

of benzaldehyde linearly increased with the reaction time up to ca. 5 h, followed by a gradual increase, suggesting that the catalyst deactivation took place. When the solid catalyst was separated by filtration at the reaction time of 3 h and the reaction was further continued by using the filtrate, the formation of benzaldehyde perfectly stopped after the separation of solid catalyst. These results clearly indicate that the oxidation of benzyl alcohol to benzaldehyde took place by the heterogeneous catalysis.

The results of both X-ray absorption (Figs. 4 and 5) and UV–vis absorption (Fig. 6) clearly showed that Ni(II) exists as well dispersed and octahedrally coordinated species by oxygen atoms in $Mg_{2.5}Ni_{0.5}Al$ HT. No Ni–O–Ni bonding exists and all Ni(II) are combined either mainly to Mg(II) or to Al(III) through oxygen bonding, suggesting that Ni(II) are well dispersed by substituting the Mg sites in Mg-Al HT. The Ni dispersion in the sample was high at the low Ni content and decreased with increasing Ni content, whereas number of the active sites increased with increasing Ni content. The balance between the Ni dispersion and the number of active sites resulted in the highest activity at the composition of $Mg_{2.5}Ni_{0.5}Al$ HT. A plausible reaction mechanism is shown in Fig. 9. At the active sites, Ni(II) cations were probably coordinated by either Mg(II) or Al(III) through oxygen bonding, in which Mg(II) as a base can donate electron to the Ni atoms through oxygen, whereas Al(III) as a Lewis acid can activate alcohols as alkoxide anions by the deprotonation. As a result, oxygen molecules are activated on the Ni(II) sites assisted by Mg(II), attack alkoxides bound to Al(III), and finally forms carbonyl compounds by the dehydrogenation. The amount of water formed well coincided with that of acetone after the oxidation of dry 2-propanol (10 mL) with molecular oxygen in the presence of $Mg_{2.5}Ni_{0.5}Al$ HT for 24 h; i.e., acetone and water were formed in the amount of 0.10 and 0.13 mmol at 356 K, and 0.24 and 0.25 mmol at 333 K, respectively. Under N_2 atmosphere, neither water nor acetone was detected. These results indicated that a simple dehydrogenation did
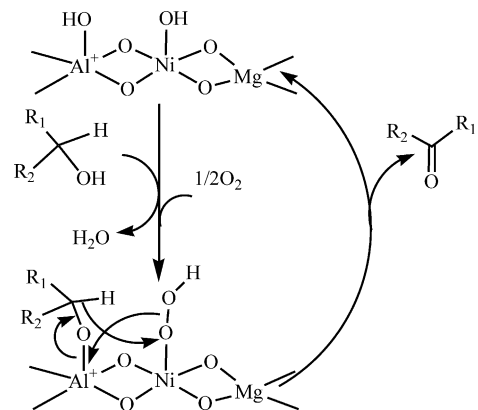
not occur [44] and might strongly suggest the reaction mechanism shown in Fig. 9.

4. Conclusion

Octahedrally coordinated and isolated Ni(II) sites formed by the Ni substitution of Mg(II) sites in Mg-Al HT and revealed a high activity in the liquid-phase oxidation of alcohols with molecular oxygen. Benzyl alcohol was the most effectively oxidized to benzaldehyde, the yield of which increased significantly with increasing nickel content up to ca. 7.6 wt%. Use of non-polar solvents, such as toluene, was favorable for this oxidation reaction. The Ni(II) incorporated inside the framework of hydrotalcite do not leach during the reaction and worked as the heterogeneous catalyst. It is likely that Ni(II) worked as the active site by activating molecular oxygen assisted by Mg(II) as a base as well as by activating alcohol on the Al(III) as a Lewis acid, and that alcohol was oxidized on the $Mg_{2.5}Ni_{0.5}Al$ HT heterogeneous catalyst.

References

[1] R.A. Sheldon, I.W.C.E. Arends, A. Dijksman, Catal. Today 57 (2000) 157.
[2] M. Hudlucky, Oxidations in Organic Chemistry, ACS Monograph Series, American Chemical Society, Washington, DC, 1990.
[3] I.E. Marko, P.R. Giles, M. Tsukazaki, S.M. Brown, C.J. Urch, Science 274 (1996) 2044.
[4] A. Dijksman, A. Marino-Gonzalez, A.M. Payeras, I.W.C.E. Arends, R.A. Sheldon, J. Am. Chem. Soc. 123 (2001) 6826.
[5] A.K. Roby, J.P. Kingsley, CHEMTECH (1996) 39.
[6] B.M. Trost, Angew. Chem. Int. Ed. Engl. 34 (1995) 259.
[7] M.K. Dalal, M.J. Upadhyay, R.N. Ram, J. Mol. Catal. A 142 (1999) 325.
[8] L.F. Liotta, A.M. Vanezia, G. Deganello, A. Longo, A. Martorana, Z. Schay, L. Guczi, Catal. Today 66 (2001) 271.
[9] N. Kakiuchi, Y. Maeda, T. Nishimura, S. Uemura, J. Org. Chem. 66 (2001) 6620.
[10] K. Yamaguchi, N. Mizuno, Angew. Chem. Int. Ed. Engl. 41 (2002) 4538.

[11] K. Kaneda, T. Yamashita, T. Matsushita, K. Ebitani, J. Org. Chem. 63 (1998) 1750.

[12] K. Ebitani, H-B. Ji, T. Mizugaki, K. Kaneda, J. Mol. Catal. A 212 (2004) 161.

[13] K. Mori, T. Hara, T. Mizugaki, K. Ebitani, K. Kaneda, J. Am. Chem. Soc. 126 (2004) 10657.

[14] V.D. Makwana, Y.-C. Son, A.R. Howell, S.L. Suib, J. Catal. 210 (2002) 46.

[15] B.M. Choudhary, M.L. Kantam, A. Rahman, C.V. Reddy, K.K. Rao, Angew. Chem. Int. Ed. Engl. 40 (2001) 763.

[16] V.R. Choudhary, R.A. Chaudhari, V.S. Narkhede, Catal. Commun. 4 (2003) 171.

[17] V.R. Choudhary, D.K. Dumbre, B.S. Uphade, V.S. Narkhede, J. Mol. Catal. A 215 (2004) 129.

[18] F. Cavani, F. Trifiro, A. Vaccari, Catal. Today 11 (1991) 173.

[19] M. Miyata, A. Okada, Clay Clay Miner. 25 (1977) 14.

[20] W.T. Reichle, J. Catal. 94 (1985) 547.

[21] D. Dollimore, G.R. Heal, J. Appl. Chem. 14 (1964) 109.

[22] K. Tanaka, H. Yamashita, R. Tsuchitani, T. Funabiki, T. Yoshida, J. Chem. Soc., Faraday Trans. 84 (1988) 2987.

[23] J.C.A.A. Roefuls, J.A. van Bokhoven, A.J. van Dillen, J.W. Geus, K.P. de Jong, Chem Eur. J. 8 (2002) 5571.

[24] J.S. Valente, F. Figueras, M. Gravelle, P. Kumbnar, J. Lopez, J.P. Besse, J. Catal. 189 (2001) 370.

[25] K. Takehira, T. Shishido, D. Shouro, K. Murakami, M. Honda, T. Kawabata, K. Takaki, Catal. Commun. 5 (2004) 209.

[26] M.A. Drezdon, Inorg. Chem. 37 (1988) 4628.

[27] F.A. Cotton, G. Wilkinson, Advanced Inorganic Chemistry, fifth ed., John Wiley & Sons, New York, 1988.

[28] G.J. Colpas, M.J. Maroney, C. Bagyinka, M. Kumar, W.S. Willis, S.L. Suib, N. Baidya, P.K. Mascharak, Inorg. Chem. 30 (1991) 920.

[29] M.P. Feth, A. Klein, H. Bertagnolli, Eur. J. Inorg. Chem. (2003) 839.

[30] G. Kwag, J.-G. Lee, H. Lee, S. Kim, J. Mol. Catal. A 193 (2003) 13.

[31] J.F. Marco, J.R. Gancedo, M. Gracia, J.L. Gautier, E. Ríos, J. Solid State Chem. 153 (2000) 74.

[32] K. Ebitani, T. Ohmatsuzawa, E. Matsunami, T. Tanaka, H. Hattori, Catal. Today 16 (1993) 447.

[33] S. Takenaka, H. Ogihara, I. Yamanaka, K. Otsuka, Appl. Catal. A. 217 (2001) 101.

[34] M.J. Holgano, V. Rives, M.S. San Román, Appl. Catal. A 214 (2001) 219.

[35] R.A. Schoonheydt, D. Roodhooft, H. Leeman, Zeolites 7 (1987) 412.

[36] M. Briend-Faure, J. Jeanjean, G. Spector, D. Delafosse, F. Bozon-Verduraz, J. Chim. Phys. Phys. -Chim. Biol. 79 (1982) 489.

[37] C. Lepetit, M. Che, J. Phys. Chem. 100 (1996) 3137.

[38] M.A. Zanjanchi, A. Ebrahimian, J. Mol. Struct. 693 (2004) 211.

[39] St.G. Christoskova, N. Danova, M. Georgieva, O.K. Argirov, D. Mehandzhiev, Appl. Catal. A 128 (1995) 219.

[40] St.G. Christoskova, M. Stoyanova, N. Danova, O. Argirov, Appl. Catal. A 173 (1998) 101.

[41] M. Stoyanova, St.G. Christoskova, M. Georgieva, Appl. Catal. A 248 (2003) 249.

[42] K. Nakagawa, R. Konaka, T. Nakata, J. Org. Chem. 27 (1962) 1597.

[43] C.J. Easton, S.K. Eichinger, M.J. Pitt, Tetrahedron 53 (1997) 5609.

[44] K. Yamaguchi, N. Mizuno, Chem. Eur. J. 9 (2003) 4353.